



Original Article

GC-MS-Based Phytochemical Analysis, *In-depth* ADMET Screening and Molecular Docking Targeting EGFR for Anticancer Potential

Ramana Hechhu¹, Karthickeyan Krishnan², Venkata Ramana Singamaneni^{3,*}, Pericharla Venkata Narasimha Raju⁴, Phanindra Erukulla⁵, Krishna Vamsi Kandimalla⁶, Ramenani Hari Babu⁷, Nithin Vidiyala^{8,*}

¹Department of Pharmaceutical Chemistry, Malla Reddy Institute of Pharmaceutical Sciences, Malla Reddy Vishwavidyapeeth (Deemed to be University), Secunderabad, 500100, Telangana, India

²Department of Pharmacy Practice, School of Pharmaceutical Sciences, Vels Institute of Science, Technology and Advanced Studies (VISTAS), Pallavaram, Chennai 600 117, India

³Department of Analytical Research and Development, Cambrex, Charles City, Iowa- 50616, United States

⁴Department of Regulatory Affairs, Hikma Pharmaceuticals USA Inc., 2 Esterbrook Lane, Cherry Hill, NJ 08003, United State

⁵Department of Regulatory Affairs, Ricon Pharma LLC, 100 Ford Rd, Suite 9, Denville, NJ 07834, United State

⁶Department of Regulatory Affairs, InvaGen Pharmaceuticals, A Cipla subsidiary, 550 South Research Place, Central Islip, NY 11722, United States

⁷Department of Pharmacy Practice, Teerthanker Mahaveer College of Pharmacy, Teerthanker Mahaveer University, Moradabad 244001, Uttar Pradesh, India

⁸Cerevel Therapeutics 222 Jacobs St. Suite 200, Boston, Massachusetts 02141, United State

ARTICLE INFO**Article history**

Submitted: 2025-12-04

Revised: 2025-12-27

Accepted: 2026-01-20

ID: CHEMM-2512-2061

DOI: [10.48309/chemm.2026.564116.2061](https://doi.org/10.48309/chemm.2026.564116.2061)

KEYWORDS

Qurs-e-Ziabetus Khas

Unani formulation

GC-MS analysis

Computational analysis

Anticancer activity

ABSTRACT

Qurs-e-Ziabetus Khas is a classical unani herbal-mineral formulation traditionally prescribed for diabetes; however, its phytochemical composition and anticancer potential remain underexplored. This study aimed to standardize QZKH and elucidate its bioactive profile with a focus on epidermal growth factor receptor (EGFR) kinase-targeted activity. QZKH tablets were evaluated for organoleptic, physicochemical, and microbial parameters, followed by preliminary phytochemical screening, gas chromatography-mass spectrometry (GC-MS) based profiling, molecular docking against EGFR (PDB ID: 7S11), and *in silico* ADMET analysis. Quality control studies confirmed acceptable pH (6.3–6.8), moisture, ash, and extractive values and the absence of foreign matter, heavy metals, pesticides, and pathogenic microbes, indicating a safe and standardized formulation. Phytochemical tests revealed carbohydrates, amino acids, fats and oils, cardiac and anthraquinone glycosides, saponins, alkaloids, phenolics, tannins, and flavonoids, supporting a strong antioxidant and metabolic regulatory potential. GC-MS analysis identified aromatic acids (benzeneacetic, hydrocinnamic), fatty acids (dodecanoic, tetradecanoic, oleic), cyclic dipeptides (cyclo (Pro-Ala), 3,6-diisopropylpiperazine-2,5-dione, phenylalanyl-leucine), long-chain amide (erucamide), and ursolic acid derivatives as key constituents. Docking studies showed that urs-12-en-23-oic acid, 3-(acetyloxy)-, methyl ester (–7.2 kcal/mol) and phenylalanyl-leucine (–5.8 kcal/mol) exhibited higher binding affinity to EGFR than the native ligand, stabilized by multiple hydrogen bonds and hydrophobic interactions. ADMET predictions highlighted cyclo (Pro-Ala), 3,6-diisopropylpiperazine-2,5-dione, hydrocinnamic acid, and benzeneacetic acid as drug-like, safe candidates with favorable pharmacokinetic and toxicity profiles. Collectively, these findings substantiate QZKH as a chemically rich, standardized formulation with promising EGFR-targeted anticancer potential, warranting further validation.

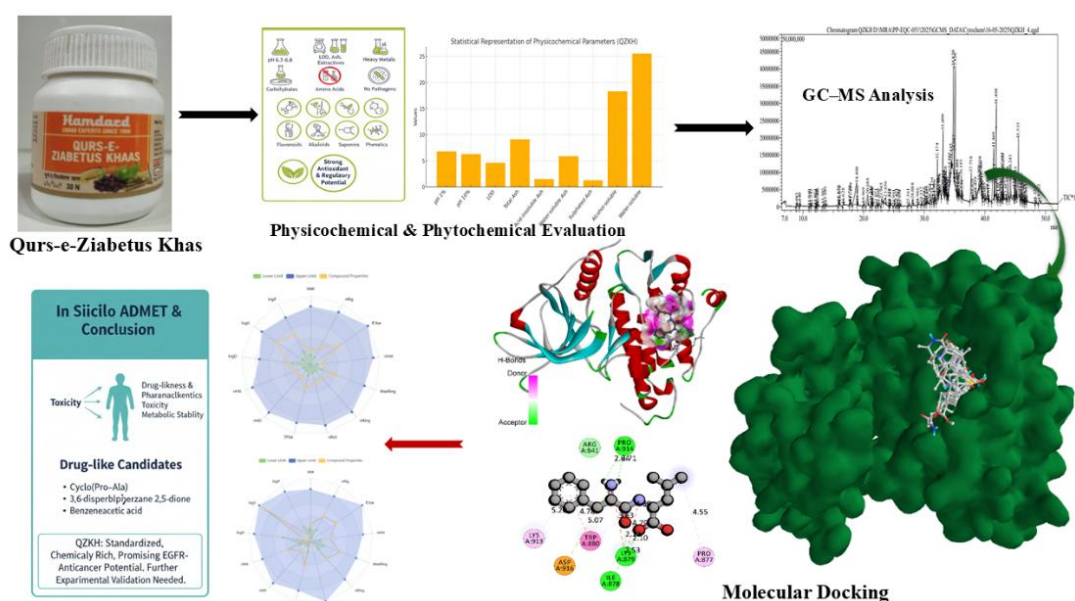
* Corresponding author: Venkata Ramana Singamaneni, Nithin Vidiyala

E-mail: ramana.singamaneni@outlook.com, nithinvidiyala@gmail.com

© 2026 by Sami Publishing Company

This is an open access article under the [CC BY](https://creativecommons.org/licenses/by/4.0/) license

GRAPHICAL ABSTRACT



Introduction

Qurs-e-Ziabetus Khas (QZKH) is a classical Unani herbal-mineral formulation traditionally prescribed for the management of Ziabetus Shakri (diabetes mellitus). Rooted in the holistic principles of Unani medicine, QZKH is composed of botanical and mineral derivatives that collectively aim to normalize blood glucose levels, strengthen metabolic functions, and restore humoral balance [1]. Beyond its well-documented antidiabetic relevance, emerging evidence suggests that many phytoconstituents present in traditional formulations possess broad pharmacological properties, including antioxidant, anti-inflammatory, immunomodulatory, and cytoprotective effects. These therapeutic attributes are of growing scientific interest due to their potential implications in chronic metabolic disorders and cancer progression, where oxidative stress and dysregulated signaling pathways play central roles [2, 3].

Among the various oncogenic pathways, the EGFR pathway is one of the most extensively studied molecular targets because it is involved in cellular proliferation, migration, survival, and angiogenesis. EGFR overexpression or mutation is commonly associated with multiple cancers, including breast, lung, colorectal, and prostate malignancies. Therefore, EGFR inhibition has become an essential strategy in targeted

anticancer therapy [4–6]. Although several synthetic EGFR inhibitors are clinically available, issues such as toxicity, drug resistance, and pharmacokinetic limitations underscore the need for safer, naturally derived alternatives. In this context, phytochemicals, particularly phenolics, flavonoids, fatty acids, glycosides, dipeptides, and triterpenoids, have attracted significant attention due to their multitargeted mechanisms and favorable safety profiles.

GC-MS remains one of the most powerful analytical tools for decoding the chemical complexity of polyherbal formulations [7–9]. Its sensitivity, resolution, and ability to detect volatile and semi-volatile compounds make it ideal for profiling diverse phytoconstituents present in traditional medicines, such as QZKH. Identifying these constituents provides a biochemical rationale for therapeutic claims and establishes a foundation for mechanistic investigation. Complementing GC-MS, molecular docking, and *in silico* pharmacokinetic (ADMET) predictions offer valuable insights into the interaction potential, drug-likeness, and safety profiles of identified compounds [10–12]. By integrating these computational assessments, it is possible to predict the phytochemicals that may serve as promising EGFR modulators.

The present study aimed to perform comprehensive GC-MS-based phytochemical

profiling of QZKH and evaluate its bioactive constituents using molecular docking against EGFR kinase, accompanied by ADMET analysis. This combined analytical and computational framework seeks to establish a scientific basis for exploring the anticancer potential of QZKH, expanding its therapeutic relevance beyond traditional antidiabetic use, while contributing to evidence-based validation of Unani medicine.

Materials and Methods

Procurement and Sample Preparation of QZKH

QZKH tablets were procured from a licensed Unani pharmacy in Hyderabad, Telangana, India, ensuring product authenticity through verification of manufacturer details, batch numbers, and expiry dates. The formulation was inspected for physical integrity and stored under dry and ambient conditions until further analysis. Ten tablets were selected for experimental processing, checked for uniformity, and pulverized into a fine powder using a clean mortar and pestle (Figure 1).



Figure 1: Sample of QZKH

The powder was sieved through a 60-mesh screen to obtain a homogeneous sample, which was stored in an airtight amber glass container to protect it from moisture and light. This standardized powdered sample served as the starting material for GC-MS-based phytochemical profiling and subsequent *in silico* evaluation against EGFR kinase to explore the potential anticancer activity of QZKH.

Physicochemical Evaluation

Physicochemical assessment of the QZKH sample was performed to confirm its quality, purity, and suitability for advanced analyses. Sensory attributes such as color, odor, and taste were examined, followed by the measurement of pH in 1% and 10% aqueous solutions using a calibrated digital pH meter. Foreign matter was isolated and quantified, and the moisture content was determined by drying the samples at 105 °C. Ash value analysis, including total ash, acid-insoluble ash, sulfated ash, and water-soluble ash, was performed to estimate the inorganic content. Alcohol and water solubilities were evaluated using 90% ethanol and chloroform. Heavy metals were quantified using atomic absorption spectrophotometry after acid digestion with 3 M HNO₃. Pesticide residues were assessed using gas chromatography, achieving detection limits of 0.1–0.5 ppb and acceptable recovery values (>80%) [13–15].

Preliminary Phytochemical and Microbial Evaluation

The formulation was subjected to preliminary phytochemical screening to identify the major classes of secondary metabolites. Standard qualitative assays were employed to detect carbohydrates and reducing sugars (Molisch's, Fehling's, Barfoed's, Benedict's tests), proteins and amino acids (Biuret, Ninhydrin, Millon's tests), oils and fats (saponification test), steroids (Salkowski and Liebermann–Burchard tests), glycosides (Keller–Killiani and Bortrager's foam tests), flavonoids (lead acetate and Shinoda tests), alkaloids (Dragendorff's, Wagner's, Mayer's, and Hager's reagents), and phenolics/tannins (ferric chloride and lead acetate tests). Positive reactions confirmed the presence of multiple bioactive constituents that are relevant to pharmacological activity [16–18].

Microbial quality assessment was performed to determine the total viable count and to detect specific pathogenic organisms. One gram of powdered sample was serially diluted and cultured using the pour plate technique on

Nutrient, MacConkey, Cetrimide, and Sabouraud dextrose agar. Bacterial plates were incubated at 37 °C for 24 h, and fungal plates were incubated at 27 °C for 72 h. Pathogen identification was carried out using selective and enrichment media: *E. coli* (MacConkey broth), *Salmonella* (DC agar after enrichment), *Shigella* (Salmonella–Shigella agar, TSI confirmation), *Pseudomonas aeruginosa* (cetrimide agar and oxidase test), and *Staphylococcus aureus* (MSA, catalase, and coagulase tests). These evaluations ensured microbial safety and confirmed the suitability of the material for further GC–MS and *in silico* analyses [19–21].

GC–MS Analysis

GC–MS was performed to identify the phytochemical constituents of QZKH. The prepared sample extract was introduced into the GC–MS system with a 1 µL injection volume under conditions optimized for phytochemical profiling. A programmed oven temperature gradient was applied to achieve the effective separation of volatile and semi-volatile components. Mass spectra were recorded in the scan mode, and each chromatographic peak was characterized based on the retention time and fragmentation patterns. Compound identification was performed by matching the acquired spectra with the NIST mass

spectral library, which enabled reliable annotation of the detected constituents. The total ion chromatogram (TIC) and peak data generated from this analysis formed the basis for establishing the phytochemical profile of the formulation [22,23].

Molecular Docking

Molecular docking was conducted to assess the interaction of the GC-MS-identified phytochemicals with EGFR kinase (PDB ID: 7SI1). Ligand structures were sketched and refined using ChemDraw and the corresponding canonical SMILES sequences were retrieved from PubChem. All the ligands were energy-minimized using PyRx (AutoDock Vina). The EGFR receptor was prepared in Discovery Studio by removing water molecules and non-essential heteroatoms, adding polar hydrogens, and applying the appropriate charges. The active site was defined using a docking grid centered at X=46.236917, Y=17.070333, and Z=-24.060167. Ligands were docked within this predefined pocket, and binding affinities and interaction profiles were obtained. The resulting poses were analyzed using Discovery Studio to identify the key bonding interactions relevant to anticancer activity [24–26]. Figure 2 shows a 3D ribbon view of the EGFR kinase enzyme.

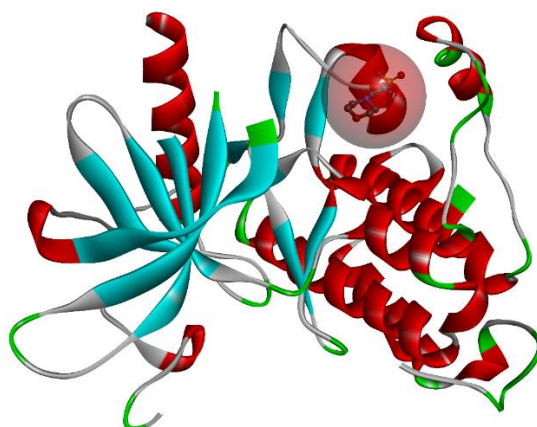


Figure 2: 3D ribbon view of EGFR kinase enzyme with active site

ADMET Analysis

ADMET profiling of the identified phytochemicals was performed to evaluate their drug-likeness and

pharmacokinetic suitability. Chemical structures were prepared using ChemDraw, verified via PubChem, and submitted to ADMETlab 3.0 for computational prediction of absorption,

distribution, metabolism, excretion, and toxicity parameters. These predictions support the selection of phytochemicals with favorable safety and pharmacokinetic characteristics for further investigation [11,12,27].

Results and Discussion

QZKH

QZKH is a Unani herbal mineral formulation used for managing diabetes (Ziabetus Shakri), which regulates blood glucose, supports pancreatic function, enhances metabolism, and provides antioxidant effects. Each tablet contains Tabasheer (73.53 mg), offering cooling and demulcent action; Satt-e-Gilo (73.53 mg), known for its immunomodulatory and hypoglycemic activity; Maghz-e-Khasta-e-Jamun (29.41 mg), which is traditionally used to control blood sugar; Gurmar Booti (14.70 mg), which suppresses sweet taste and supports insulin function; and Kushta-e-Zamurrud (29.41 mg), which contributes to metabolic and antioxidant benefits. Laoob-e-Aspaghol (*Plantago ovata*, Q.S.) provides soluble fiber that slows carbohydrate absorption and helps maintain glycemic control.

Organoleptic, Physicochemical, and Microbial Analysis of QZKH

QZKH tablets were evaluated for organoleptic, physicochemical, and microbial quality attributes. Organoleptically, the tablets were gray, had a characteristic herbal odor, were tasteless with slight astringency, and showed a smooth, hard, and compact texture. Physicochemical assessment indicated near-neutral pH values (6.8 for 1% and 6.3 for 10% solutions), the absence of foreign matter, and an acceptable moisture level (LOD 4.6%). Ash values—total (9.1%), acid-insoluble (1.5%), water-soluble (5.9%), and sulfated (1.3%)—were within permissible limits, reflecting the appropriate inorganic content (Figure 3). Extractive values were 18.3% (alcohol-soluble) and 25.56% (water-soluble), demonstrating good solubility of the phytoconstituents, while heavy metals and pesticide residues were absent, confirming the safety of the sample. Microbial analysis further ensured product quality, with no detectable pathogenic organisms, including *E. coli*, *Salmonella*, *Shigella*, *Pseudomonas aeruginosa*, and *Staphylococcus aureus*, indicating compliance with the microbiological safety standards.

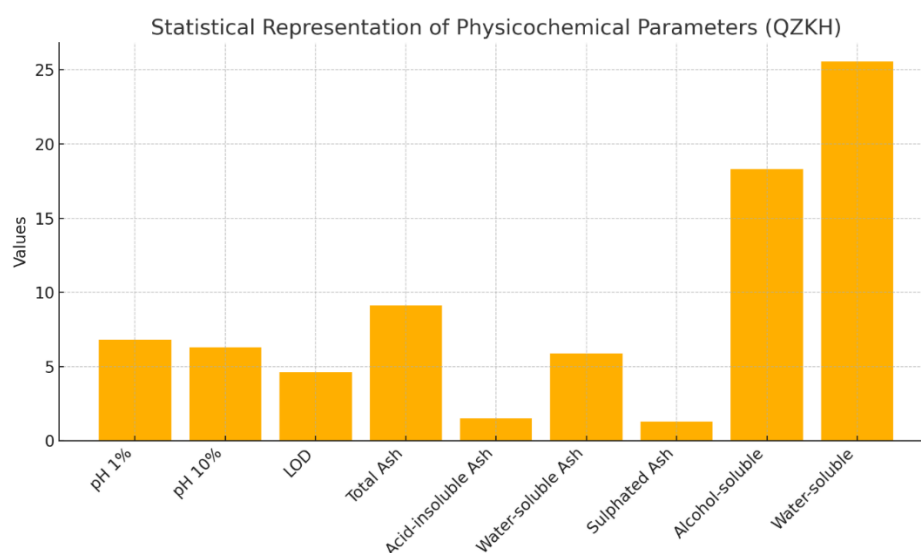


Figure 3: The physicochemical analysis of QZKH

Preliminary Phytochemical Screening

Preliminary phytochemical analysis of the QZKH tablets revealed the presence of a diverse range of bioactive constituents, highlighting the

therapeutic potential of the formulation. As shown in Table 1, carbohydrates, reducing sugars, and monosaccharides tested positive, indicating the presence of basic nutritional and energy-yielding

components that may contribute to the metabolic support. Proteins and amino acids were also detected, suggesting the presence of nitrogenous compounds that may aid in cellular functions and tissue repair. Fats and oils were also present, reflecting the inclusion of lipid-based constituents, which may support the absorption of lipophilic phytochemicals. Cardiac glycosides and anthraquinone glycosides showed positive outcomes, demonstrating the presence of compounds with potential cardiogenic, laxative, or antioxidant activities, depending on their structural nature. Saponin glycosides, which are known for their roles in cholesterol regulation, immune modulation, and antidiabetic effects, were also detected.

Alkaloids were moderately present (++), indicating significant levels of nitrogen-containing

secondary metabolites with potential antihyperglycaemic, anti-inflammatory, and antioxidant properties. Phenolic compounds and tannins showed a notable abundance (+++ for tannins), emphasizing the strong presence of antioxidant constituents that can reduce oxidative stress, a key factor in diabetes management. Similarly, flavonoids were abundant (+++), reinforcing their well-documented roles in glycemic control, enzyme inhibition, free radical scavenging, and anti-inflammatory actions. Steroids were absent, indicating the lack of steroidal constituents in the formulation. Overall, the phytochemical profile confirmed that QZKH tablets contain multiple bioactive classes that contribute synergistically to their antidiabetic, antioxidant, and metabolic regulatory effects.

Table 1: The results of preliminary phytochemical screening of QZKH tablets

Chemical Test	Observations
Test for carbohydrates	+
Test for reducing sugars	+
Test for monosaccharides	+
Test for proteins	+
Test for amino acids	+
Test for fats and oil	+
Test for steroids	-
Test for cardiac glycosides	+
Test for anthraquinone glycosides	+
Test for saponin glycoside	+
Test for alkaloids	++
Test for phenolic compounds	+
Test for tannins	+++
Test for Flavonoids	+++

+++ = abundant; ++ = moderately present; + = trace/low presence; --- = strongly absent; -- = moderately absent; and -= absent

GC-MS Analysis

GC-MS profiling of the QZKH sample revealed a chemically diverse spectrum of phytoconstituents, highlighting the complex herbal nature of the formulation. Multiple peaks were detected within a retention time window of approximately 18–50 min, representing both low- and high-molecular-

weight compounds (Table 2 and Figure 4). The identification process relied on NIST20 library matching, retention time comparisons, and fragmentation pattern interpretation. Aromatic acids were a major component of the profile. Benzeneacetic acid (6.79%) and hydrocinnamic acid (1.61%) exhibited strong spectral matches and characteristic fragments, indicating reliable

identification. These aromatic acids are well known for their antimicrobial, anti-inflammatory, and antioxidant activities, suggesting a potential role in the biological effects of QZKH. Several fatty acids have also been identified, including dodecanoic acid, tetradecanoic acid, and oleic acid,

each showing diagnostic McLafferty rearrangement ions typical of saturated and unsaturated fatty acids. Their presence suggests contributions to membrane-stabilizing, antimicrobial, and anti-inflammatory effects within the formulation.

Table 2: GC-MS identified compounds in QZKH sample

Peak No.	Retention time (min)	Compound identified	Molecular formula	Area %	Reported bioactivity
15	18.898	Benzeneacetic acid	C ₈ H ₈ O ₂	6.79	Antimicrobial and anti-inflammatory
18	20.688	Hydrocinnamic acid	C ₉ H ₁₀ O ₂	1.61	Antioxidant
33	28.088	Dodecanoic acid	C ₁₂ H ₂₄ O ₂	0.69	Antimicrobial
40	31.339	Cyclo(Pro-Ala)	C ₈ H ₁₂ N ₂ O ₂	0.88	Bioactive cyclic dipeptide
43	32.174	Tetradecanoic acid	C ₁₄ H ₂₈ O ₂	3.02	Antimicrobial
57	34.183	3,6-Diisopropylpiperazine-2,5-dione	C ₁₀ H ₁₈ N ₂ O ₂	1.83	Cyclic dipeptide
66	36.115	Oleic acid	C ₁₈ H ₃₄ O ₂	1.19	Anti-inflammatory
79	41.469	Phenylalanyl-leucine	C ₁₄ H ₂₂ N ₂ O ₃	8.06	Antioxidant and regulatory peptide
96	45.535	Erucamide	C ₂₂ H ₄₃ NO	4.51	Anti-inflammatory, analgesic
105	48.952	Ursolic acid derivative	C ₃₃ H ₅₄ O ₄	0.61	Anti-inflammatory and hepatoprotective

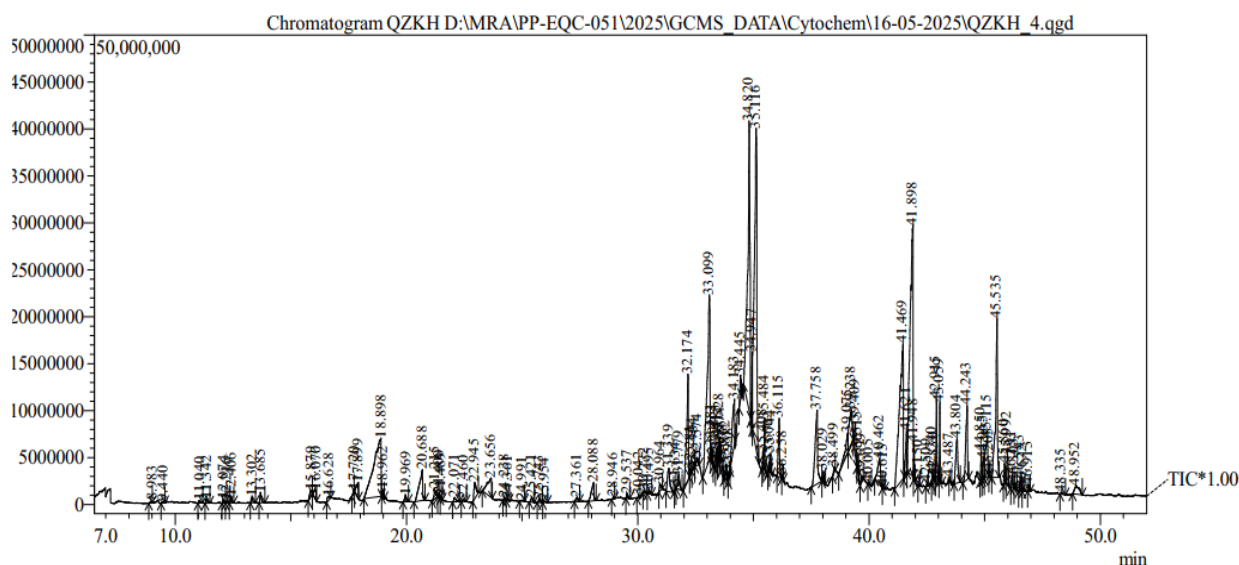


Figure 4: GC-MS graph of QZKH sample

A particularly notable feature of the chromatogram was the detection of cyclic dipeptides (diketopiperazines), such as cyclo(Pro-Ala), 3,6-diisopropylpiperazine-2,5-dione, and phenylalanyl-leucine (8.06%). These compounds displayed distinct fragmentation ions corresponding to proline, valine, and leucine

residues, confirming their cyclic nature. Diketopiperazines are known for their strong antioxidant, cytoprotective, and antimicrobial properties, indicating their relevance in the therapeutic potential of QZKH. The chromatogram also contained 13-docosenamide (erucamide) (4.51%), a long-chain fatty acid amide identified

through characteristic amide ion fragments and high spectral similarity. Erucamide is recognized for its anti-inflammatory and analgesic effects, which support its contribution to the bioactivity of the formulation. Moreover, the presence of an ursolic acid derivative, although in low abundance (0.61%), indicated the presence of high-molecular-weight triterpenoids typical of medicinal plants and was associated with hepatoprotective and anti-inflammatory actions. Overall, GC-MS analysis confirmed that QZKH contains a rich mixture of aromatic acids, fatty acids, cyclic dipeptides, long-chain amides, and triterpenoid derivatives. These constituents collectively support the traditional therapeutic applications of QZKH via antimicrobial, antioxidant, cytoprotective, and anti-inflammatory mechanisms.

Molecular Docking

Molecular docking analysis of phytochemicals identified in QZKH against EGFR kinase (PDB ID: 7SI1) demonstrated significant binding affinities through diverse interactions within the active site pocket (Table 3). The 2D and 3D docking interactions are shown in Figure 4. The native ligand exhibited a docking score of -4.5 kcal/mol, forming key hydrogen bonds with PRO914, ILE878, and LYS879, alongside alkyl interactions with ALA920. This established reference pattern served as a benchmark for comparing the test compounds. Among the screened phytochemicals, Urs-12-en-23-oic acid, 3-(acetyloxy)-, methyl ester exhibited the strongest binding affinity (-7.2 kcal/mol), surpassing the native ligand and all other compounds. The high number of hydrogen bonds (notably with ARG803) combined with multiple hydrophobic interactions involving LEU799, LYS879, LYS913, ALA920, ILE878, and TRP880 suggest strong anchoring within the EGFR ATP-binding cleft. The extensive alkyl and π -alkyl contacts further indicated stabilizing van der Waals interactions, supporting its potential as a lead EGFR inhibitor.

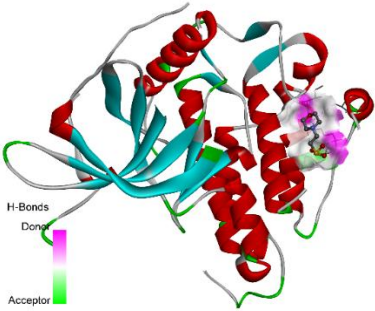
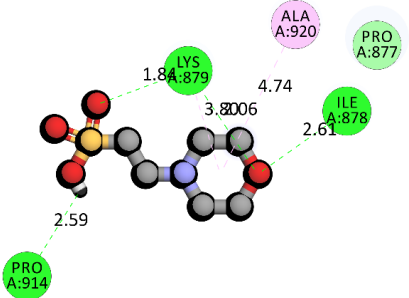
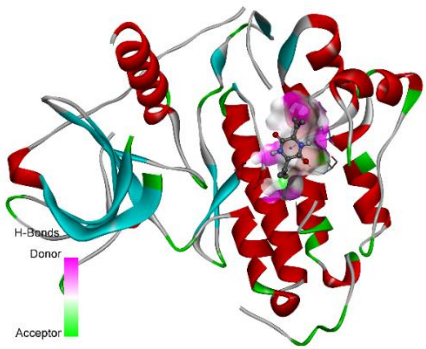
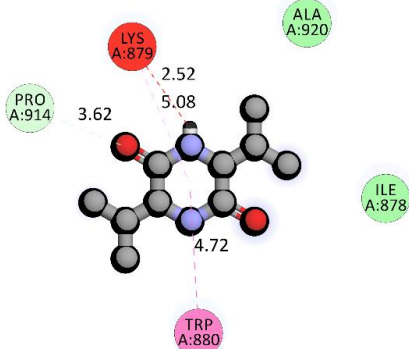
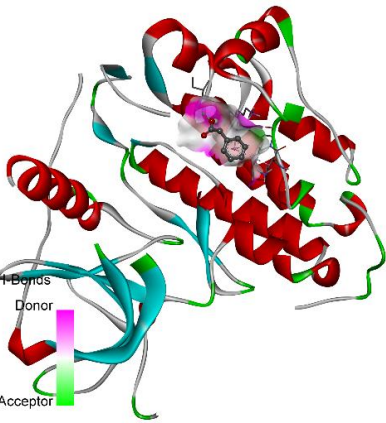
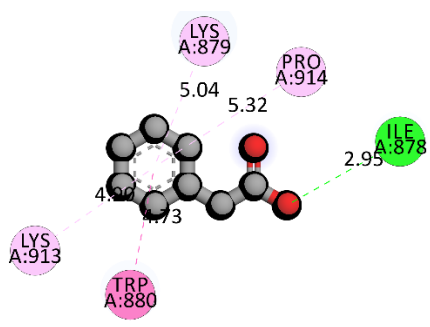
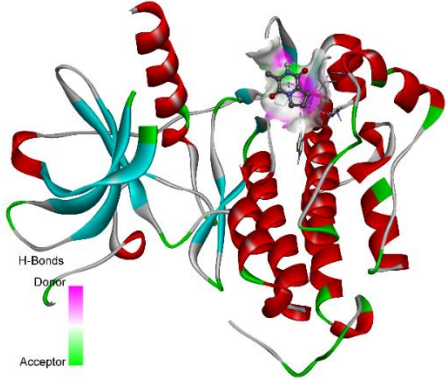
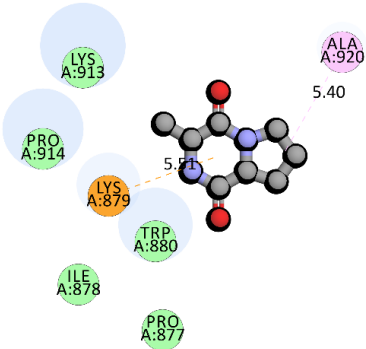
Phenylalanyl-leucine showed the second-best docking score (-5.8 kcal/mol), forming a critical electrostatic attractive charge interaction with ASP916, followed by several hydrogen bonds with PRO914, ILE878, and LYS879. This combination of electrostatic and hydrogen-bonding interactions, along with aromatic stacking with TRP880, implies a strong and specific engagement with catalytic residues, enhancing the inhibitory potential. Compounds such as 3,6-diisopropylpiperazine-2,5-dione, hydrocinnamic acid, and benzenecetic acid exhibited moderate binding scores (from -4.8 to -4.4 kcal/mol). These molecules primarily interacted via π - π T-shaped and π -alkyl interactions with TRP880 and LYS913, suggesting that aromatic stabilization plays a critical role in EGFR binding. Hydrogen bonding with PRO914 and ILE878 further contributed to their moderate affinity. Fatty acids, including oleic acid, tetradecanoic acid, and dodecanoic acid, displayed docking scores ranging from -4.5 to -4.2 kcal/mol. Their binding is largely mediated through hydrophobic alkyl interactions with residues such as PRO877, LEU799, ALA920, and TRP880. Although these interactions support stable fitting in the hydrophobic pocket, the absence of strong polar contacts may limit their overall binding affinity compared to that of more interactive ligands. Cyclo(Pro-Ala) exhibited a docking score of -4.1 kcal/mol, driven by π -donor hydrogen bonding with ILE878 and hydrophobic interactions with PRO877 and TRP880. While these contacts suggest moderate activity, they remain weaker than those observed with more potent ligands.

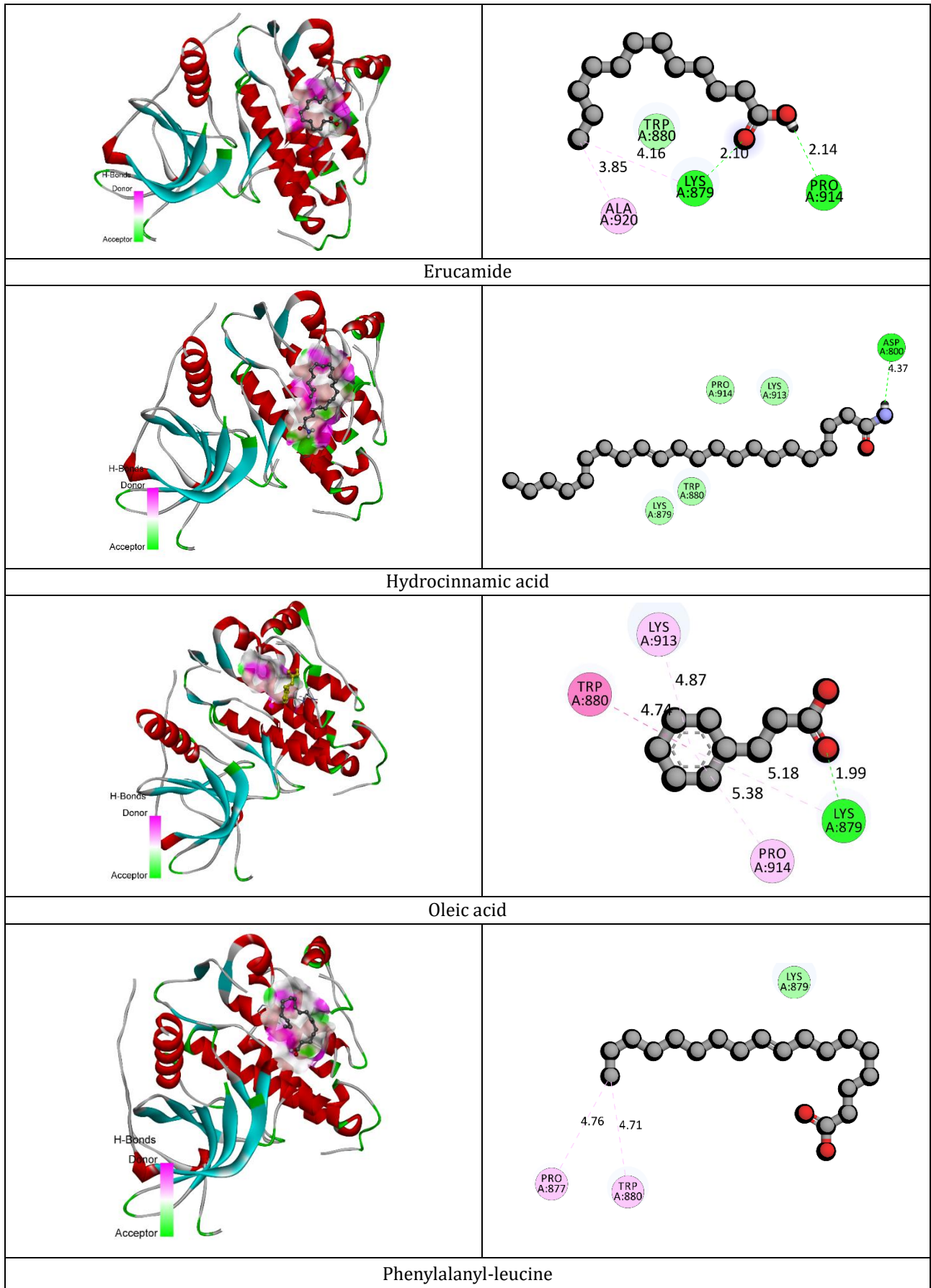
Overall, the docking results indicated that the urs-12-en-23-oic acid derivative, followed by phenylalanyl-leucine, showed the highest potential for EGFR kinase inhibition due to its strong binding energies, extensive hydrogen bonding, and stable hydrophobic interactions. These findings highlight the key phytoconstituents of QZKH as promising candidates for anticancer activity via EGFR modulation and warrant further *in vitro* and *in vivo* validation.

Table 3: Binding interactions of selected compounds with EGFR kinase enzyme

Amino acid	Bond length	Bond type	Bond category	Ligand energy	Docking score
				(Kcal/mol)	
Native ligand					
PRO914	2.59146	Hydrogen bond	Conventional hydrogen bond	563.70	-4.5
ILE878	2.60926				
LYS879	2.0615				
LYS879	1.84099				
LYS879	3.79924	Hydrophobic	Alkyl		
ALA920	4.73572				
3,6-Diisopropylpiperazine-2,5-dione					
PRO914	3.62181	Hydrogen bond	Carbon hydrogen bond	260.78	-4.8
TRP880	4.71659	Hydrophobic	π - π T-shaped		
LYS879	5.08434		π -Alkyl		
Benzeneacetic acid					
ILE878	2.9457	Hydrogen bond	Conventional hydrogen bond	78.26	-4.4
TRP880	4.72739	Hydrophobic	π - π T-shaped		
LYS879	5.04294		π -Alkyl		
LYS913	4.89988		π -Alkyl		
PRO914	5.31637		π -Alkyl		
Cyclo(Pro-Ala)					
ILE878	3.07252	Hydrogen bond	π -Donor hydrogen bond	201.06	-4.1
PRO877	3.50772	Hydrophobic	π -Sigma		
LYS879	4.28325		Alkyl		
ALA920	5.40303				
TRP880	5.46189				
Dodecanoic acid					
PRO914	2.14495	Hydrogen bond	Conventional hydrogen bond	3.94	-4.2
LYS879	2.10012				
LYS879	4.15736	Hydrophobic	Alkyl		
ALA920	3.84689				
Erucamide					
ASP800	2.17274	Hydrogen bond	Conventional hydrogen bond	37.99	-4.5
Hydrocinnamic acid					
LYS879	1.99093	Hydrogen bond	Conventional hydrogen bond	67.27	-4.8
TRP880	4.73895	Hydrophobic	π - π T-shaped		
LYS879	5.17855	Hydrophobic	π -Alkyl		
LYS913	4.87286				
PRO914	5.37723				

Oleic acid						
PRO877	4.75896	Hydrophobic	Alkyl	70.58	-4.5	
TRP880	4.7081	Hydrophobic	π -Alkyl			
Phenylalanyl-leucine						
ASP916	5.0709	Electrostatic	Attractive Charge	434.27	-5.8	
PRO914	2.63884	Hydrogen bond	Conventional hydrogen bond			
PRO914	2.71404					
ILE878	2.53164					
LYS879	2.09549					
TRP880	4.7816	Hydrophobic	π - π T-shaped			
PRO877	4.55169		Alkyl			
TRP880	4.59533		π -Alkyl			
Tetradecanoic acid						
VAL876	2.63842	Hydrogen bond	Conventional hydrogen bond	3.05	-4.3	
LEU799	5.18009	Hydrophobic	Alkyl			
LYS913	4.44648		π -Alkyl			
TRP880	5.17836					
Urs-12-en-23-oic acid, 3-(acetyloxy)-, methyl ester						
ARG803	2.07303	Hydrogen bond	Conventional hydrogen bond	563.7	-7.2	
LEU799	4.92229	Hydrophobic	Alkyl			
LYS913	4.80529					
LYS913	4.11692					
LYS879	5.11004					
ALA920	3.64701					
ILE878	4.21125					
ALA920	3.82681					
LYS879	3.58223					
LYS913	4.71612					
LYS879	5.39641					
LYS913	4.82495					
ALA920	3.99156					
TRP880	5.39264					π -Alkyl
TRP880	4.50441					

3D Interaction	2D Interaction
Native Ligand	
 <p>3D interaction diagram of the Native Ligand. The protein structure is shown as a ribbon model with red and cyan segments. The ligand is shown as a stick model in purple. A legend indicates H-Bonds (Donor in pink, Acceptor in green).</p>	 <p>2D interaction diagram of the Native Ligand. The ligand is shown as a stick model. Interactions with amino acid residues are shown as dashed lines with distances: LYS A:879 (1.84), ALA A:920 (4.74), PRO A:877 (2.61), ILE A:878 (2.61), and PRO A:914 (2.59).</p>
3,6-Diisopropylpiperazine-2,5-dione	
 <p>3D interaction diagram of 3,6-Diisopropylpiperazine-2,5-dione. The protein structure is shown as a ribbon model. The ligand is shown as a stick model in purple. A legend indicates H-Bonds (Donor in pink, Acceptor in green).</p>	 <p>2D interaction diagram of 3,6-Diisopropylpiperazine-2,5-dione. The ligand is shown as a stick model. Interactions with amino acid residues are shown as dashed lines with distances: LYS A:879 (2.52), ALA A:920 (3.62), PRO A:914 (3.62), ILE A:878 (4.72), and TRP A:880 (5.08).</p>
Benzeneacetic acid	
 <p>3D interaction diagram of Benzeneacetic acid. The protein structure is shown as a ribbon model. The ligand is shown as a stick model in purple. A legend indicates H-Bonds (Donor in pink, Acceptor in green).</p>	 <p>2D interaction diagram of Benzeneacetic acid. The ligand is shown as a stick model. Interactions with amino acid residues are shown as dashed lines with distances: LYS A:879 (5.04), PRO A:914 (5.32), ILE A:878 (2.95), LYS A:913 (4.90), and TRP A:880 (4.73).</p>
Cyclo(Pro-Ala)	
 <p>3D interaction diagram of Cyclo(Pro-Ala). The protein structure is shown as a ribbon model. The ligand is shown as a stick model in purple. A legend indicates H-Bonds (Donor in pink, Acceptor in green).</p>	 <p>2D interaction diagram of Cyclo(Pro-Ala). The ligand is shown as a stick model. Interactions with amino acid residues are shown as dashed lines with distances: ALA A:920 (5.40), LYS A:913 (5.71), PRO A:914 (5.71), LYS A:879 (5.71), TRP A:880 (5.71), ILE A:878 (5.71), and PRO A:877 (5.71).</p>
Dodecanoic acid	



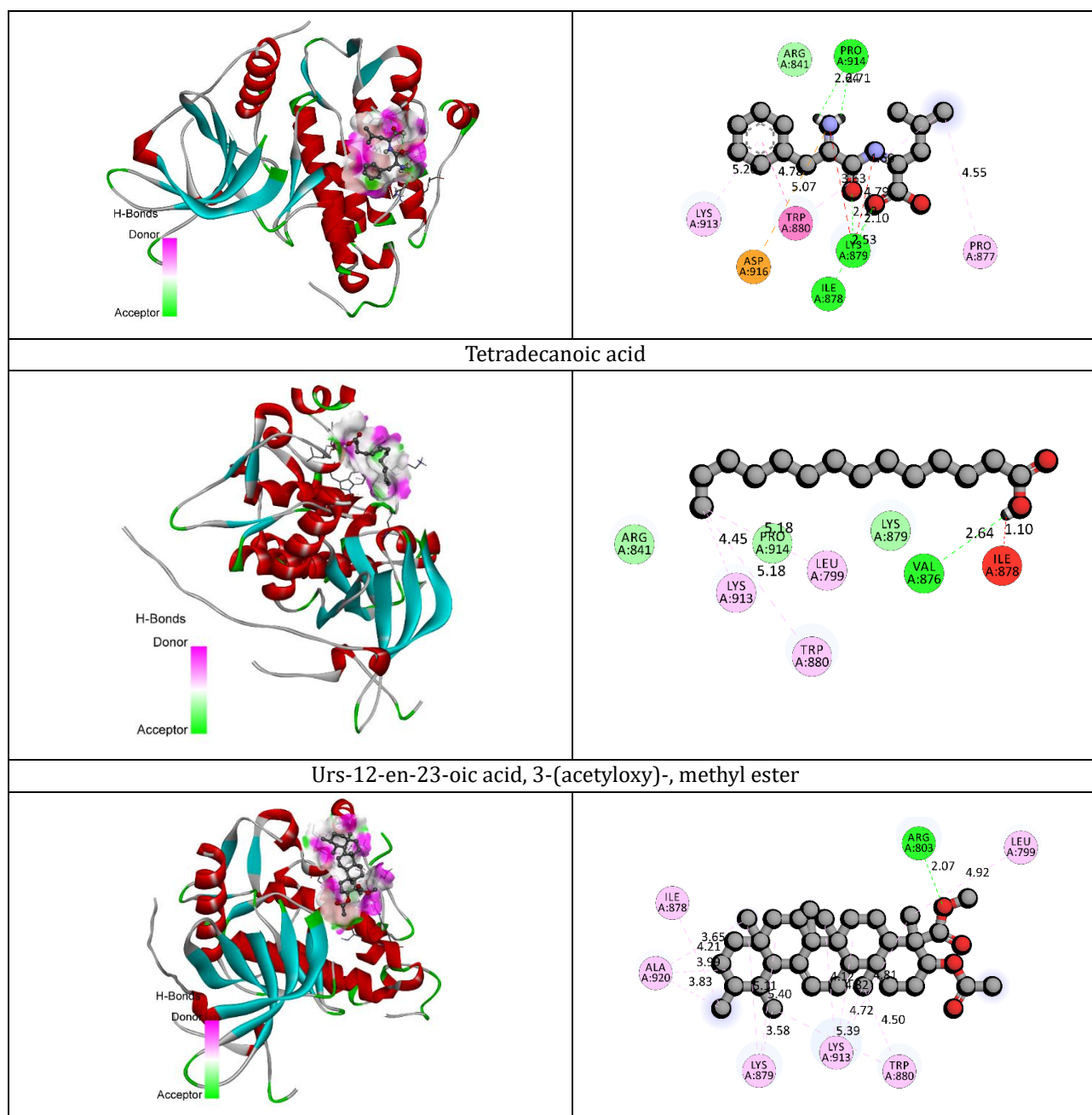


Figure 4: 2D and 3D docking interactions of the identified compounds and native ligands with EGFR kinase

ADMET Analysis

The ADMET and drug-likeness profiling of QZKH phytoconstituents against EGFR kinase (7SI1) showed that several compounds exhibited properties comparable to, or in some aspects better than, the native ligand, while others presented significant developability liabilities.

Table 4 shows physicochemical properties of selected compounds. In terms of physicochemical behavior, the native ligand is a small, polar, and hydrophilic molecule (MW 195.06, TPSA 66.84, logP -1.51, and logS -1.12), consistent with good

aqueous solubility but limited membrane permeability. Most phytoconstituents are more lipophilic (positive logP) and slightly larger, which may favor target binding but can compromise solubility and metabolic profile. Short-chain and peptidomimetic compounds such as 3,6-diisopropylpiperazine-2,5-dione (MW 198.14, TPSA 58.2, and logP 0.14) and cyclo(Pro-Ala) (MW 168.09, TPSA 49.41, logP -0.63) remain close to the native ligand range and balance polarity and lipophilicity better than long-chain fatty acids and the triterpenoid ester.

Table 4: Physicochemical properties of selected compounds

Compounds	logP	logS	TPSA	nRing	nRot	nHD	nHA	Dense	Volume	MW
Native ligand	-1.51265	-1.12381	66.84	1	3	1	5	1.158021	168.4426	195.06
3,6-Diisopropylpiperazine-2,5-dione	0.138879	-1.03875	58.2	1	2	2	4	0.955993	207.2609	198.14
Benzeneacetic acid	1.518644	-1.17206	37.3	1	2	1	2	0.935679	145.4025	136.05
Cyclo(Pro-Ala)	-0.63263	0.001974	49.41	2	0	1	4	1.024237	164.1125	168.09
Dodecanoic acid	4.803721	-3.9944	37.3	0	10	1	2	0.866384	231.0523	200.18
Erucamide	6.56323	-4.09052	43.09	0	19	2	2	0.83584	403.5822	337.33
Hydrocinnamic acid	1.89683	-1.46267	37.3	1	3	1	2	0.922381	162.6985	150.07
Oleic acid	7.062676	-5.86546	37.3	0	15	1	2	0.84969	332.1917	282.26
Phenylalanyl-leucine	-0.19993	-1.55704	92.42	1	8	4	5	0.944126	294.6217	278.16
Tetradecanoic acid	5.723228	-4.87761	37.3	0	12	1	2	0.859081	265.6442	228.21
Urs-12-en-23-oic acid, 3-(acetyloxy)-, and methyl ester	5.479295	-6.10765	52.6	5	4	0	4	0.908826	563.7932	512.39

Hydrocinnamic acid and benzenoacetic acid also maintain moderate molecular weights and low TPSA, with logP values (1.90 and 1.52, respectively) compatible with passive diffusion. In contrast, erucamide, oleic, dodecanoic, tetradecanoic acids and the ursane-type ester are highly lipophilic (logP > 4.5) with relatively low polarity, which may predispose to poor aqueous solubility and extensive tissue/lipid binding.

Drug-like indices further supported this distinction (Table 5). The native ligand showed a QED value of 0.598, with no Lipinski, Pfizer, GSK, or chelator rule violations, indicating a balanced oral drug profile. Several small phytochemicals displayed equal or superior QED values:

hydrocinnamic acid (0.712), phenylalanyl-leucine (0.698), 3,6-diisopropylpiperazine-2,5-dione (0.669), and benzenoacetic acid (0.665), all with zero Lipinski/Pfizer/GSK violations and favorable Golden Triangle flags. Cyclo(Pro-Ala) also showed an acceptable QED (0.53) with clean rule profiles. In contrast, the highly lipophilic fatty acids (dodecanoic, tetradecanoic, oleic acid, and erucamide) and the urs-12-en-23-oic acid methyl ester trigger Pfizer and GSK rule alerts, and the ursane derivative additionally violates Lipinski, indicating a higher risk of poor oral pharmacokinetics and off-target liabilities despite its high NP score.

Table 5: Drug-likeness properties of designed derivatives

Compounds	QED	NP score	Lipinski rule	Pfizer rule	GSK rule	Golden triangle	Chelator rule
Native ligand	0.598	-1.198	0	0	0	1	0
3,6-Diisopropylpiperazine-2,5-dione	0.669	1.123	0	0	0	1	0
Benzenoacetic acid	0.665	-0.164	0	0	0	1	0
Cyclo(Pro-Ala)	0.53	1.141	0	0	0	1	0
Dodecanoic acid	0.541	0.495	0	1	1	0	0
Erucamide	0.199	0.475	0	1	1	0	0
Hydrocinnamic acid	0.712	0.139	0	0	0	1	0
Oleic acid	0.291	0.869	0	1	1	0	0
Phenylalanyl-leucine	0.698	0.224	0	0	0	0	0
Tetradecanoic acid	0.488	0.433	0	1	1	0	0
Urs-12-en-23-oic acid, 3-(acetyloxy), and methyl ester	0.28	3.067	1	1	1	1	0

Absorption predictions revealed that the native ligand possessed high human intestinal absorption (HIA 0.91) and reasonable oral bioavailability proxies (F20%, F30%, and F50% = 0.98, 0.95, and 0.63) (Table 6). Among the phytoconstituents, cyclo(Pro-Ala) and 3,6-diisopropylpiperazine-2,5-dione showed broadly comparable or slightly favorable oral profiles. Cyclo(Pro-Ala) displayed a high HIA (0.93) and excellent predicted fractions absorbed at higher thresholds (F30% 0.95, F50% 0.99), suggesting better oral exposure than the native ligand. 3,6-Diisopropylpiperazine-2,5-dione showed good HIA (0.85) and markedly higher F50% (0.98), but

it is predicted to be a strong P-gp inhibitor (0.996) and weak substrate, which may promote drug-drug interactions and affect efflux at the intestinal barrier. Urs-12-en-23-oic acid methyl ester, despite very low HIA (5.79E-05), exhibits a high F50% (0.99), suggesting that once absorbed, its systemic exposure can be substantial, but uptake is likely limited and formulation-dependent. Simple aromatic acids, such as benzenoacetic and hydrocinnamic acids, display very low HIA values, reflecting their ionizable and hydrophilic nature at physiological pH, leading to poor predicted oral absorption relative to the native ligand.

Table 6: Absorption parameter of selected compounds

Compounds	Caco-2 permeability	MDCK permeability	Pgp-inhibitor	Pgp-substrate	HIA	F20%	F30%	F50%
Native ligand	-4.95317	-4.59541	0.000139	0.000895	0.905602	0.978309	0.954305	0.626995
3,6-Diisopropylpiperazine-2,5-dione	-5.04322	-4.74073	0.996353	0.008006	0.851717	0.302486	0.838805	0.980731
Benzeneacetic acid	-4.82381	-4.26619	1.76E-05	0.007081	0.000204	0.001173	0.00039	0.00729
Cyclo(Pro-Ala)	-5.30962	-4.70566	0.743436	0.800839	0.9268	0.766006	0.95202	0.98615
Dodecanoic acid	-5.09852	-4.77514	6.10E-05	0.024496	0.626665	0.44178	0.683438	0.239138
Erucamide	-5.12315	-4.74832	0.014108	0.001091	0.003972	0.11894	0.571917	0.403486
Hydrocinnamic acid	-4.29508	-4.61644	0.18274	0.016576	0.005374	0.011204	0.05324	0.242211
Oleic acid	-5.08101	-4.71704	0.002651	0.000155	0.141995	0.286498	0.721989	0.374845
Phenylalanyl-leucine	-6.03388	-4.66096	2.02E-05	0.907759	0.000924	0.188595	0.132363	0.597047
Tetradecanoic acid	-5.09766	-4.78904	3.58E-05	0.018977	0.756654	0.604258	0.837822	0.32716
Urs-12-en-23-oic acid, 3-(acetyloxy)-, and methyl ester	-5.16657	-4.89598	0.999507	0.004642	5.79E-05	0.67433	0.561444	0.991317

The distribution and metabolism parameters further discriminate suitable leads, as shown in Table 7. The native ligand showed low plasma protein binding (PPB 10.5%) and a high unbound fraction (Fu 87.8%), favoring wide tissue distribution and efficient target engagement. Cyclo(Pro-Ala) and 3,6-diisopropylpiperazine-2,5-dione behaved similarly, with a low PPB (8.9% and 20.7%) and high Fu (88.6% and 72.2%), close to or within the range of the native ligand. In contrast, long-chain fatty acids and erucamide were highly bound (PPB > 96%, Fu < 1%), indicating restricted free concentrations and potential depot-like behavior in lipid-rich tissues. The triterpenoid ester showed intermediate PPB (~94%) but a high Fu (~6.33%), suggesting a modestly higher free fraction than fatty acids

despite its high lipophilicity. CYP interaction profiles suggest that most small, polar phytoconstituents resemble the native ligand in presenting low to moderate probabilities of acting as CYP inhibitors or substrates, thereby minimizing the risk of metabolic interaction. Compounds such as erucamide and oleic acid show very high probabilities of interacting with multiple CYP isoforms (particularly CYP3A4), and dodecanoic/tetradecanoic acids are predicted to be strong CYP3A4 substrates, which can predispose to variable clearance and drug-drug interactions. The ursane derivative also showed very high substrate probabilities across several CYPs, indicating a complex metabolic fate distinct from the relatively clean profile of the native ligand.

Table 7: Distribution and metabolism parameter of selected molecules

Compounds	Distribution				Metabolism									
	PPB%	VD	BBB	Fu	CYP1A2		CYP2C19		CYP2C9		CYP2D6		CYP3A4	
					Inhibitor	Substrate	Inhibitor	Substrate	Inhibitor	Substrate	Inhibitor	Substrate	Inhibitor	Substrate
Native Ligand	10.52185	-0.44374	0.011683	87.79532	1.56E-09	9.11E-10	2.59E-09	1.89E-06	3.14E-06	0.137909	4.75E-07	1.23E-08	1.43E-08	3.48E-06
3,6-Diisopropylpiperazine-2,5-dione	20.68165	-0.25624	1.44E-05	72.18765	0.000136	0.01207	0.029427	0.957346	0.000117	0.102995	0.000296	0.005189	0.022636	0.053851
Benzeneacetic acid	84.41633	-0.61334	0.278441	12.87706	0.007617	0.00598	0.008822	0.001841	0.042731	0.365265	0.000225	0.001785	1.35E-05	0.059231
Cyclo(Pro-Ala)	8.909712	-0.21501	0.012657	88.62496	0.000153	0.00067	0.019075	0.831994	5.36E-06	0.041758	9.65E-06	0.046896	0.005716	0.096651
Dodecanoic acid	96.85933	0.276761	0.063945	2.688211	0.050098	0.000107	0.009364	0.097488	0.160296	0.99998	0.122798	0.539477	1.03E-05	5.58E-05

Erucamide	98.5854	0.429428	0.055684	0.555318	0.971369	1.23E-06	0.998678	0.001393	0.000142	0.999649	0.102834	0.997367	0.128705	2.19E-06
Hydrocinnamic acid	96.46359	-0.44049	0.095308	3.204833	0.001258	0.000787	0.003265	0.001064	0.014737	0.998878	0.008055	0.284985	4.70E-07	0.001947
Oleic acid	98.28009	-0.58651	0.018328	0.536366	0.997933	3.67E-08	0.998977	1.92E-05	0.010889	1	0.245062	0.980627	6.37E-05	1.04E-07
Phenylalanyl-leucine	52.56066	-0.34121	0.001503	51.96386	2.23E-12	1.27E-12	3.52E-08	4.77E-07	3.15E-09	0.023623	3.28E-09	0.243417	8.26E-08	3.97E-10
Tetradecanoic acid	97.44871	0.418707	0.035986	2.108519	0.071367	7.71E-05	0.014434	0.060129	0.16592	0.999988	0.14053	0.712885	1.24E-05	6.21E-05
Urs-12-en-23-oic acid, 3-(acetyloxy)-, methyl ester	94.1011	-0.12002	0.964683	6.330868	7.38E-05	0.315554	0.713508	0.999883	0.913603	0.997724	0.324272	0.026477	0.999609	0.999614

Excretion and toxicity predictions support the safety of several phytochemicals while highlighting potential risks to others (Table 8). The native ligand presented moderate plasma clearance (CL 3.13) and half-life (T1/2 1.57) with intermediate hepatotoxicity (H-HT 0.47) and DILI (0.34) probabilities and low-to-moderate mutagenic (Ames) and systemic toxicity indicators. Dodecanoic, tetradecanoic, and oleic acids, as well as erucamide, generally exhibited lower DILI and Ames scores than the native ligand, suggesting a lower risk of hepatotoxicity and genotoxicity, although their high lipophilicity and extensive binding remain a concern. Cyclo(Pro-Ala) and 3,6-diisopropylpiperazine-2,5-dione showed acceptable clearance and half-life values, with hepatotoxicity and DILI probabilities comparable to or slightly better than those of the native ligand, supporting their safety as potential leads. Despite favorable QED, phenylalanyl-leucine displays higher hepatotoxicity and DILI probabilities, which may limit its translational

appeal. Overall, none of the compounds presented extreme red flags in skin sensitization, carcinogenicity, eye toxicity, or respiratory toxicity relative to the native ligand, although individual profiles differed.

Environmental toxicity assessments indicated that most molecules exhibited low to moderate bioaccumulation factors (BCF), aligned with acceptable environmental profiles, as shown in Table 9. Cyclo(Pro-Ala) showed negative BCF and relatively modest LC₅₀ values, suggesting minimal bioaccumulation and manageable aquatic toxicity. The ursane-type ester had the highest BCF (2.13), indicating a higher tendency for bioaccumulation, but also high LC₅₀ values (lower acute aquatic toxicity), reflecting a trade-off between persistence and toxicity. Long-chain fatty acids display intermediate BCF values and relatively benign LC₅₀ predictions, although their hydrophobicity may favor partitioning into sediments or biota compared to the native ligand.

Table 8: Excretion and toxicity parameters of selected compounds

Compounds	Excretion		Toxicity									
	CL-plasma	T1/2	H-HT	DILI	Ames Toxicity	Rat Oral Acute Toxicity	FDAMDD	Skin Sensitization	Carcinogenicity	Eye Corrosion	Eye Irritation	Respiratory Toxicity
Native Ligand	3.130993	1.569414	0.469496	0.335374	0.28344	0.135196	0.155216	0.814554	0.362087	0.949128	0.945511	0.492139
3,6-Diisopropylpiperazine-2,5-dione	7.491855	0.613969	0.531088	0.102325	0.109581	0.282783	0.037009	0.196785	0.302397	0.000283	0.116137	0.109811
Benzeneacetic acid	0.906381	1.698027	0.369499	0.911299	0.135538	0.369164	0.027665	0.89729	0.197153	0.985346	0.997869	0.377341
Cyclo(Pro-Ala)	5.290208	2.597151	0.697301	0.300294	0.296551	0.303717	0.373506	0.134223	0.419464	0.00257	0.36261	0.22827
Dodecanoic acid	3.461065	0.763313	0.411146	0.209119	0.082866	0.143906	0.15901	0.790633	0.318141	0.983674	0.997376	0.870283
Erucamide	5.202782	0.608659	0.304089	0.006863	0.085512	0.078529	0.209968	0.999795	0.153131	0.979141	0.990684	0.907645
Hydrocinnamic acid	3.30652	1.467829	0.395799	0.108411	0.184788	0.185892	0.143563	0.453633	0.234441	0.897896	0.994139	0.377091
Oleic acid	3.49975	0.75405	0.25589	0.009204	0.088136	0.080827	0.21532	0.998412	0.135301	0.995462	0.995975	0.789521
Phenylalanyl-leucine	5.418124	1.36749	0.834808	0.691644	0.231285	0.422161	0.429232	0.916973	0.04937	0.001696	0.557234	0.334731

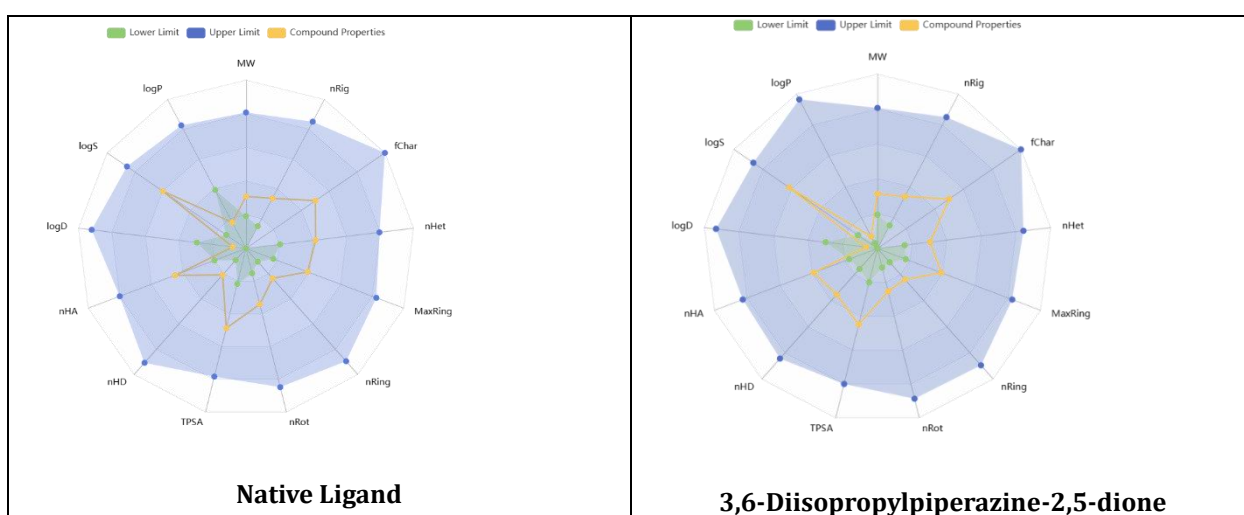
Tetradecanoic acid	3.6228	0.807519	0.417041	0.198111	0.062635	0.133879	0.168436	0.859654	0.293324	0.983424	0.997437	0.90617
Urs-12-en-23-oic acid, 3-(acetyloxy)-, and methyl ester	8.452927	0.194795	0.674222	0.473943	0.171965	0.433506	0.707243	0.915942	0.963155	0.033249	0.510118	0.702248

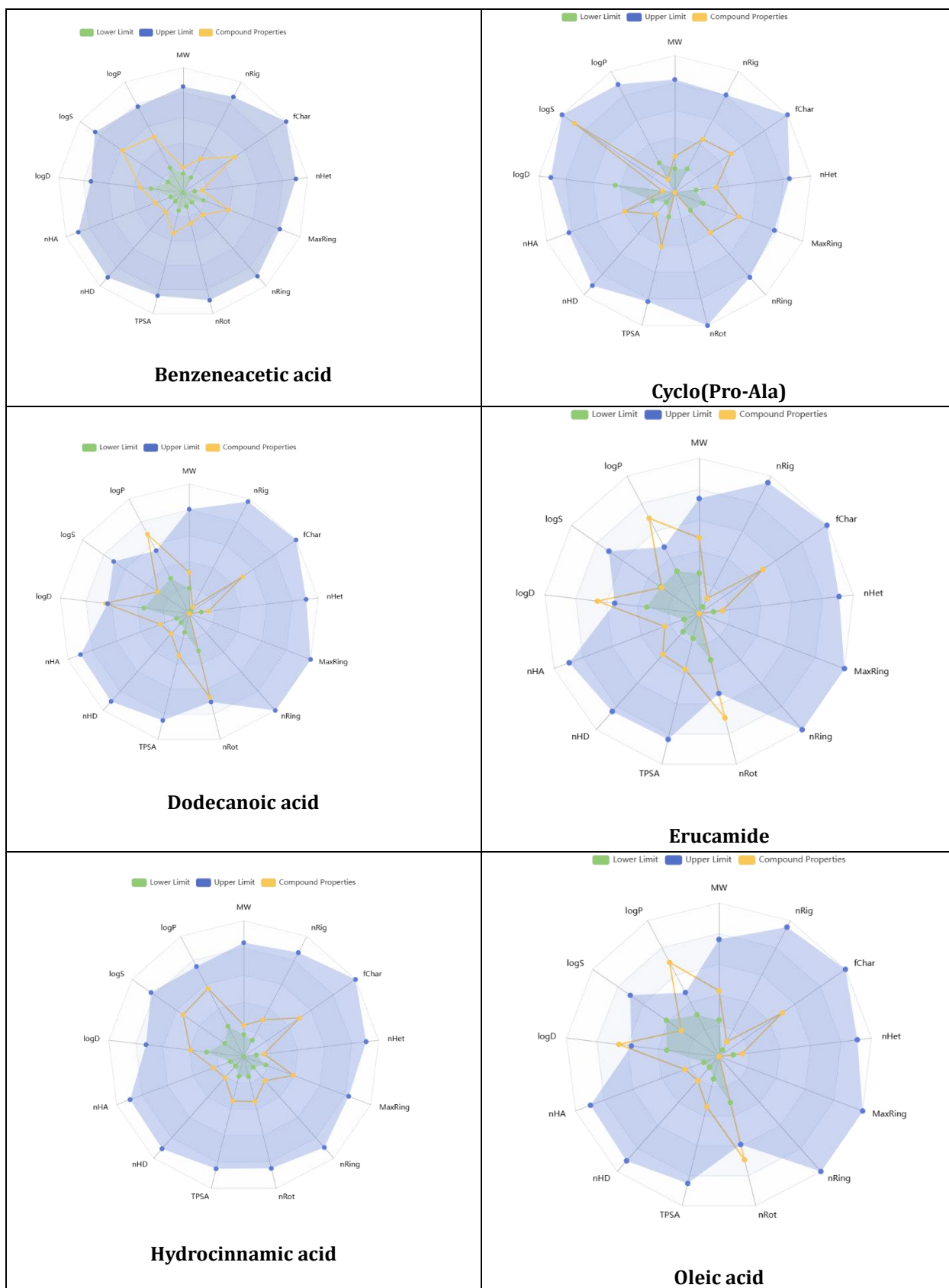
Table 9: Environmental toxicity profile of designed molecules

Compounds	BCF	IGC ₅₀	LC ₅₀ FM	LC ₅₀ DM
Native ligand	0.250029	2.065045	2.56339	3.079917
3,6-Diisopropylpiperazine-2,5-dione	0.025043	2.336337	3.086236	3.515929
Benzeneacetic acid	0.155867	2.411207	2.765902	3.353576
Cyclo(Pro-Ala)	-0.06717	1.558965	1.875355	4.077042
Dodecanoic acid	1.084779	3.846345	2.353326	5.221425
Erucamide	0.838402	4.721478	4.095908	6.143295
Hydrocinnamic acid	0.177709	2.788499	3.163065	3.752216
Oleic acid	0.79806	3.878176	1.531399	5.503197
Phenylalanyl-leucine	0.171028	2.915032	3.423095	4.221163
Tetradecanoic acid	0.924433	3.812916	1.753523	5.366167
Urs-12-en-23-oic acid, 3-(acetyloxy)-, and methyl ester	2.131132	4.40536	5.253608	5.57734

The ADMET radars of the potent compounds are listed in Figure 5. Collectively, the *in silico* ADMET data suggest that among the QZKH constituents, 3,6-diisopropylpiperazine-2,5-dione, cyclo(Pro-Ala), hydrocinnamic acid, and benzeneacetic acid most closely emulate or improve upon the drug-like and safety profile of the native EGFR ligand, particularly in terms of molecular size, polarity, lipophilicity, and overall rule compliance. Cyclo(Pro-Ala) and 3,6-diisopropylpiperazine-

2,5-dione have emerged as especially promising leads because of their balanced absorption, high unbound fraction, acceptable metabolic liability, and manageable toxicity indices, while the larger lipophilic species (fatty acids and urs-12-en-23-oic acid methyl ester) may be better viewed as secondary or formulation-dependent candidates, potentially contributing to EGFR modulation but with less favorable developability compared to the native ligand.





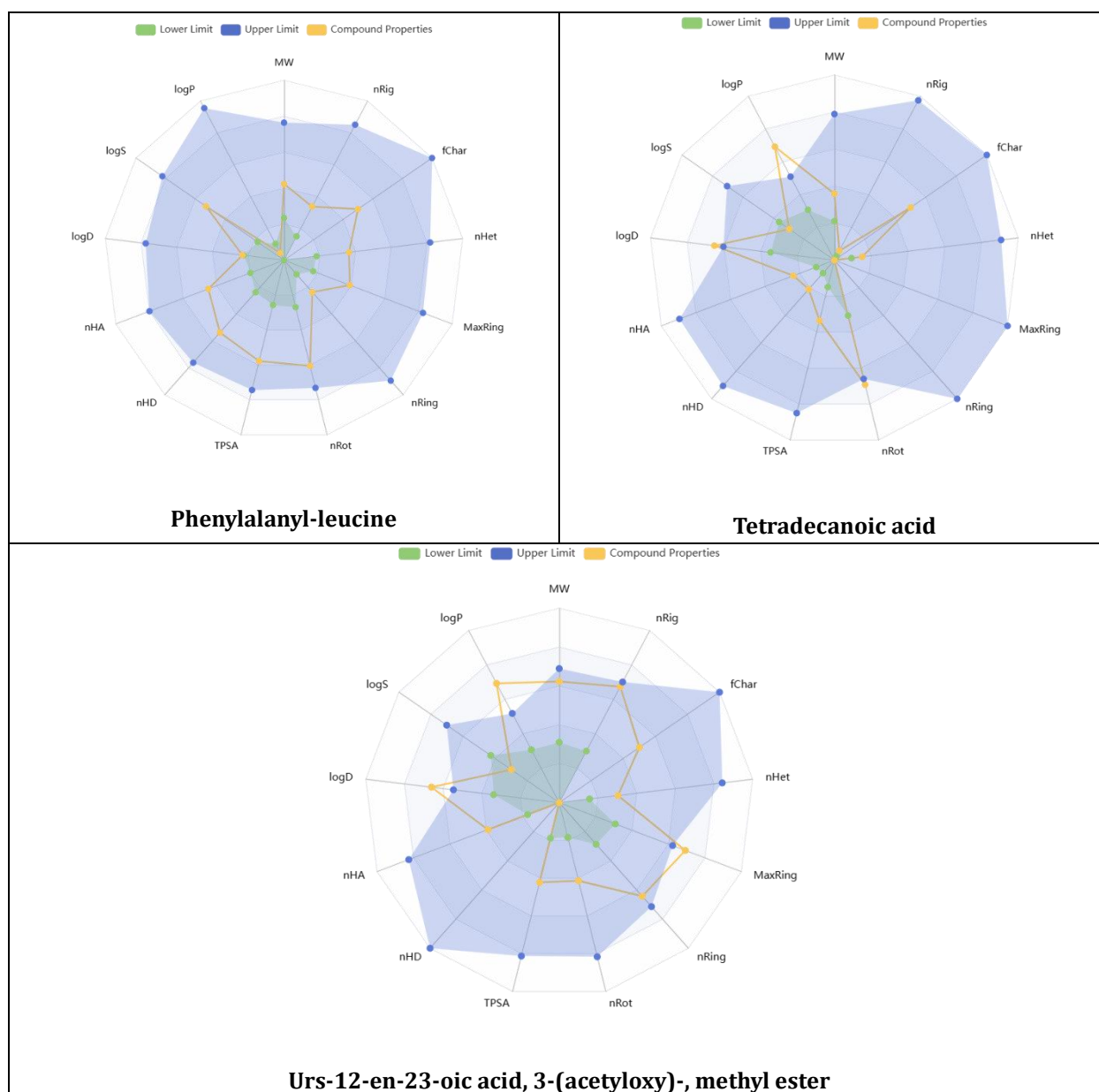


Figure 5: ADMET radar of identified compounds and native ligand

Conclusion

In conclusion, the present study comprehensively evaluated QZKH, a Unani herbal mineral formulation traditionally used for diabetes management and scientifically substantiated its multifaceted therapeutic potential. Standardization through organoleptic, physicochemical, and microbial assessments confirmed acceptable quality attributes, including near-neutral pH, suitable moisture content, permissible ash values, good extractive profiles, and the absence of foreign matter, heavy metals, pesticides, and pathogenic microbes, indicating a safe and well-processed formulation. Preliminary phytochemical

screening and GC-MS analysis revealed a rich spectrum of bioactive constituents, such as carbohydrates, amino acids, phenolics, tannins, flavonoids, saponins, aromatic acids, fatty acids, cyclic dipeptides, long-chain amides, and ursolic acid derivatives, collectively supporting antidiabetic, antioxidant, anti-inflammatory, and cytoprotective activities. Molecular docking against EGFR (PDB ID: 7SI1) highlighted urs-12-en-23-oic acid derivatives and phenylalanyl-leucine as promising EGFR modulators with better binding affinity than the native ligand, while ADMET profiling identified cyclo(Pro-Ala), 3,6-diisopropylpiperazine-2,5-dione, hydrocinnamic

acid, and benzenoacetic acid as drug-like and relatively safe candidates. Overall, these integrated experimental and *in silico* findings justify the traditional use of QZKH and suggest its potential repositioning as a complementary therapeutic candidate for diabetes and EGFR-mediated complications, warranting further *in vitro* and *in vivo* validation.

ORCID

Ramana Hechhu

<https://orcid.org/0000-0002-3865-4611>

Karthickeyan Krishnan

<https://orcid.org/0000-0002-1709-730X>

Venkata Ramana Singamaneni

<https://orcid.org/0009-0006-4328-8253>

Pericharla Venkata Narasimha Raju

<https://orcid.org/0009-0003-2259-6693>

Phanindra Erukulla

<https://orcid.org/0009-0001-2900-2881>

Krishna Vamsi Kandimalla

<https://orcid.org/0009-0004-4526-6045>

Ramenani Hari Babu

<https://orcid.org/0009-0006-6396-2110>

Nithin Vidiyala

<https://orcid.org/0009-0005-3241-1669>

References

- [1] Ansari, A.P., Nasir, A. Therapeutic effect of 'Qurs-i-Ziabetes Khas' in diabetes mellitus—a case report. *Journal of Ayurvedic and Herbal Medicine*, **2020**, 6(1), 4-8.
- [2] Eqbal, K., Alam, M.A., Quamri, M.A., Sofi, G., Ahmad Bhat, M.D. Efficacy of Qurs-e-Gulnar in Ziabetes (type 2 Diabetes Mellitus): A single blind randomized controlled trial. *Journal of Complementary and Integrative Medicine*, **2021**, 18(1), 147-153.
- [3] Hamiduddin, M., Ali, W., Jahangeer, G., Al, A. Unani formulations for management of diabetes: An overview. *International Journal of Green Pharmacy*, **2018**, 12(4), S769-783.
- [4] Onguru, O., Scheithauer, B.W., Kovacs, K., Vidal, S., Jin, L., Zhang, S., Lloyd, R.V. Analysis of epidermal growth factor receptor and activated epidermal growth factor receptor expression in pituitary adenomas and carcinomas. *Modern pathology*, **2004**, 17(7), 772-780.
- [5] Bethune, G., Bethune, D., Ridgway, N., Xu, Z. Epidermal growth factor receptor (EGFR) in lung cancer: An overview and update. *Journal of Thoracic Disease*, **2010**, 2(1), 48.
- [6] Wee, P., Wang, Z. Epidermal growth factor receptor cell proliferation signaling pathways. *Cancers*, **2017**, 9(5), 52.
- [7] Lisec, J., Schauer, N., Kopka, J., Willmitzer, L., Fernie, A.R. Gas chromatography mass spectrometry-based metabolite profiling in plants. *Nature Protocols*, **2006**, 1(1), 387-396.
- [8] Gould, O., Nguyen, N., Honeychurch, K.C. New applications of gas chromatography and gas chromatography-mass spectrometry for novel sample matrices in the forensic sciences: a literature review. *Chemosensors*, **2023**, 11(10), 527.
- [9] Valdez, C.A. Gas chromatography-mass spectrometry analysis of synthetic opioids belonging to the fentanyl class: A review. *Critical Reviews in Analytical Chemistry*, **2022**, 52(8), 1938-1968.
- [10] Khan, S.L., Bakshi, V. LC-HRMS and *in silico* Analysis Of Ailanthus Excelsa Metabolites Targeting EGFR triple mutation (L858R/T790M/C797S), *Advanced Journal of Chemistry, Section A*. **2026**, 9(2), 292-311.
- [11] Gandla, K., Islam, F., Zehravi, M., Karunakaran, A., Sharma, I., Haque, M.A., Nainu, F. Natural polymers as potential P-glycoprotein inhibitors: Pre-ADMET profile and computational analysis as a proof of concept to fight multidrug resistance in cancer. *Heliyon*, **2023**, 9(9), 19454.
- [12] Suryawanshi, R.M., Shimpi, R.B., Muralidharan, V., Nemade, L.S., Gurugubelli, S., Baig, S., Sweilam, S.H. Adme, toxicity, molecular docking, molecular dynamics, glucokinase activation, dpp-iv, α -amylase, and α -glucosidase inhibition assays of mangiferin and friedelin for antidiabetic potential. *Chemistry & Biodiversity*, **2025**, 22(5), e202402738.
- [13] Sarraf, M., Sani, A.M., Atash, M.M.S. Physicochemical, organoleptic characteristics and image analysis of the doughnut enriched with oleaster flour. *Journal of Food Processing and Preservation*, **2017**, 41(4), e13021.
- [14] Pirzada, A.S., Khan, H., Alam, W., Darwish, H.W., Elhenawy, A.A., Kuznetsov, A., Daglia, M. Physicochemical properties, pharmacokinetic studies, DFT approach, and antioxidant activity of nitro and chloro indolinone derivatives. *Frontiers in Chemistry*, **2024**, 12, 1360719.
- [15] Siraj, M.B. Quality control and phytochemical validation of *Saussurea lappa* (Costus/Qust). *International Journal of Green Pharmacy (IJGP)*, **2020**, 14(1), 38-43.
- [16] Sharma, M., Abid, R., Sajgotra, M. Phytochemical screening and thin layer chromatography of *Ficus carica* leaves extract. *Pharmaceutical and Biosciences Journal*, **2017**, 18-23.

- [17] Parvatikar, P.P., Madagi, S. Preliminary phytochemical analysis and biological screening of *Indigofera hochestetteri*. *The Pharma Innovation Journal*, **2018**, 7(3):503-5.
- [18] Ahmad, N., Shakil, A., Shinwari, Z.K., Ahmad, I., Wahab, A. Phytochemical study and antimicrobial activities of extracts and its derived fractions obtained from *Berberis vulgaris* L. and *Stellaria media* L. leaves. *Pakistan Journal of Botany*, **2022**, 54(4), 1517-1521.
- [19] Sevindik, M., Rasul, A., Hussain, G., Anwar, H., Zahoor, M.K., Sarfraz, I., Selamoglu, Z. Determination of anti-oxidative, anti-microbial activity and heavy metal contents of *Leucoagaricus leucothites*. *Pakistan Journal of Pharmaceutical Sciences*, **2018**, 31(5 Supplement), 2163-2168.
- [20] Sharma, P., Rathore, P., Choudhary, Y., Tatwade, Y., Joshi, A. Anti-microbial activity of seed oils & protein estimation of seed-content in *Clitoria ternatea*, *Lagenaria siciraria* & *Ziziphus mauritiana*. *Brazilian Journal of Science*, **2023**, 2(8), 41-46.
- [21] Nurani, L.H., Kumalasari, E., Zainab, Z., Mursyidi, A., Widayarni, S., Rohman, A. The determination of metal content, microbial contamination and dissolution assessment of the ethanol extract of pasak bumi root. *Jurnal Pharmacia*, **2017**, 7, 295-304.
- [22] Xu, F., Wei, W., Shan, X., Wang, R., Liu, L. Identification and characterization of novel synthetic cannabinoid ethyl-2-(1-(5-fluoropentyl)-1H-indole-3-carboxamido)-3, 3-dimethylbutanoate (5F-EDMB-PICA). *Forensic Toxicology*, **2022**, 40(1), 163-172.
- [23] Rani, R., Sharma, D., Chaturvedi, M., Yadav, J.P. Phytochemical analysis, antibacterial and antioxidant activity of *Calotropis procera* and *Calotropis gigantea*. *The Natural Products Journal*, **2019**, 9(1), 47-60.
- [24] Ahmed, S., Tabassum, P., Falak, S., Ahmad, A., Shaikh, M. Molecular docking and network pharmacology: Investigating vitis vinifera phytoconstituents as multi-target therapeutic agents against breast cancer. *Journal of Pharmaceutical Sciences and Computational Chemistry*, **2025**, 1(2), 116-134.
- [25] Siddiqui, F., Makhlofi, R., Salah, M.E.-S., Mohamed, E., Hojjati, M. Computational exploration of quinine and mefloquine as potential anti-malarial agents. *Journal of Pharmaceutical Sciences and Computational Chemistry*, **2025**, 1(2), 106-115.
- [26] Tamboli, A., Tayade, S. In-depth investigation of berberine and tropane through computational screening as possible DPP-IV inhibitors for the treatment of T2DM. *Journal of Pharmaceutical Sciences and Computational Chemistry*, **2025**, 1(1), 1-11.
- [27] Khan, A., Unnisa, A., Sohel, M., Date, M., Panpaliya, N., Saboo, S.G., Khan, S. Investigation of phytoconstituents of *enicostemma littorale* as potential glucokinase activators through molecular docking for the treatment of type 2 diabetes mellitus. *In Silico Pharmacology*, **2021**, 10(1), 1.



HOW TO CITE THIS ARTICLE

R. Hechhu, K. Krishnan, V. Singamaneni, P.V.N. Raju, P. Erukulla, K.V. Kandimalla, R.H. Babu, N. Vidiyala, GC-MS-Based Phytochemical Analysis, *In-depth* ADMET Screening and Molecular Docking Targeting EGFR for Anticancer Potential, *Chem. Methodol.*, 2026, 10(5) 465-488
DOI: <https://doi.org/10.48309/chemm.2026.564116.2061>
URL: https://www.chemmethod.com/article_239344.html